Measurement of Regional Myocardial Perfusion in Man with ^{133}Xenon and a Scintillation Camera

PAUL J. CANNON, RALPH B. DELL, and EDWARD M. DWYER, JR.

From the Departments of Medicine and Pediatrics, College of Physicians and Surgeons, Columbia University and the Roosevelt Hospital, New York, New York 10032

ABSTRACT A method was devised to quantitate regional capillary perfusion in the human heart by measuring the clearance constants (k) of Xenon-133 washout from multiple areas of the myocardium with a multiple-crystal scintillation camera. In 17 subjects, ^{133}Xe was injected into the right or left coronary artery or both and counts per second (cps) were recorded simultaneously on magnetic tape from each of 294 scintillation crystals viewing the precordium through a multichannel collimator. Data were processed by a digital computer. Crystals detecting the myocardial washout of ^{133}Xe were distinguished from those monitoring pulmonary excretion by positioning radioactive markers at the cardiac margins, and by a computer printout of the peak cps recorded by each crystal and its time after isotope injection into the coronary artery. The slopes of the initial segment of the multiple ^{133}Xe curves obtained in each study were calculated by the method of least squares using a monoexponential model. Myocardial blood flow rates in the cardiac regions viewed by the individual crystals were calculated (assuming a blood to myocardium partition coefficient of 0.72) along with the SD of every flow measurement. The pattern of myocardial perfusion rates so obtained was superimposed over a tracing of the subject's coronary arteriogram. Scintiphotographs showing the arrival and washout of isotope from various regions of myocardium and the area of tissue perfused by each coronary artery were obtained by replaying the data tape on an oscilloscope. Significant regional variations in local myocardial perfusion rates were observed in hearts with normal coronary arteries. When capillary flow measurements from crystals overlying the various cardiac chambers were averaged in each subject, the mean myocardial blood flow rate of the left ventricle in 17 patients, 64.1 ±13.9 (SD) ml/100 g·min, significantly exceeded that of the right ventricle, 47.8 ±10.9 ml/100 g·min, and of the right atrial region, 33.6 ±10.3 ml/100 g·min. The approach may facilitate more objective assessment of: myocardial capillary perfusion in patients with angina pectoris, the pharmacology of antianginal drugs, and the efficacy of surgical procedures to revascularize ischemic myocardium.

INTRODUCTION

Application of newer therapeutic interventions (1–6) to the extensive population of patients with coronary atherosclerosis (7–8) has been retarded by the absence of techniques to quantitatively assess regional myocardial blood flow in intact man. Coronary cineradiography is widely used diagnostically to localize constrictions or occlusions of large or medium-sized coronary vessels (9). However, radiographic visualization of the diseased artery does not provide information concerning the capillary blood flow in the region of the myocardium distal to the lesion. Furthermore, neither the adequacy of collateral blood flow beyond a coronary occlusion, nor the possibility of coronary small vessel disease (9) can be accurately assessed by arteriography alone.

The present report describes a method for quantifying capillary perfusion in various regions of the human myocardium at the time of coronary arteriography. This approach, an extension of a technique previously developed in the dog (10), consists of the injection of ^{133}Xe selectively into a coronary artery and the external measurement of isotope wash-out curves from multiple discrete regions of the myocardium with a multiple-crystal scintillation camera. The method simultaneously measures the rate constants of ^{133}Xe washout from multiple

An abstract of part of this work has been published in the *J. Clin. Invest.* **49**: 16 a. 1970.

Dr. Cannon is a recipient of Research Career Development Award 5 K3 HE 15031-07 and Dr. Dell is a recipient of Research Career Development Award 5 K3 GM 19779 from the U. S. Public Health Service.

Received for publication 2 February 1971 and in revised form 4 August 1971.

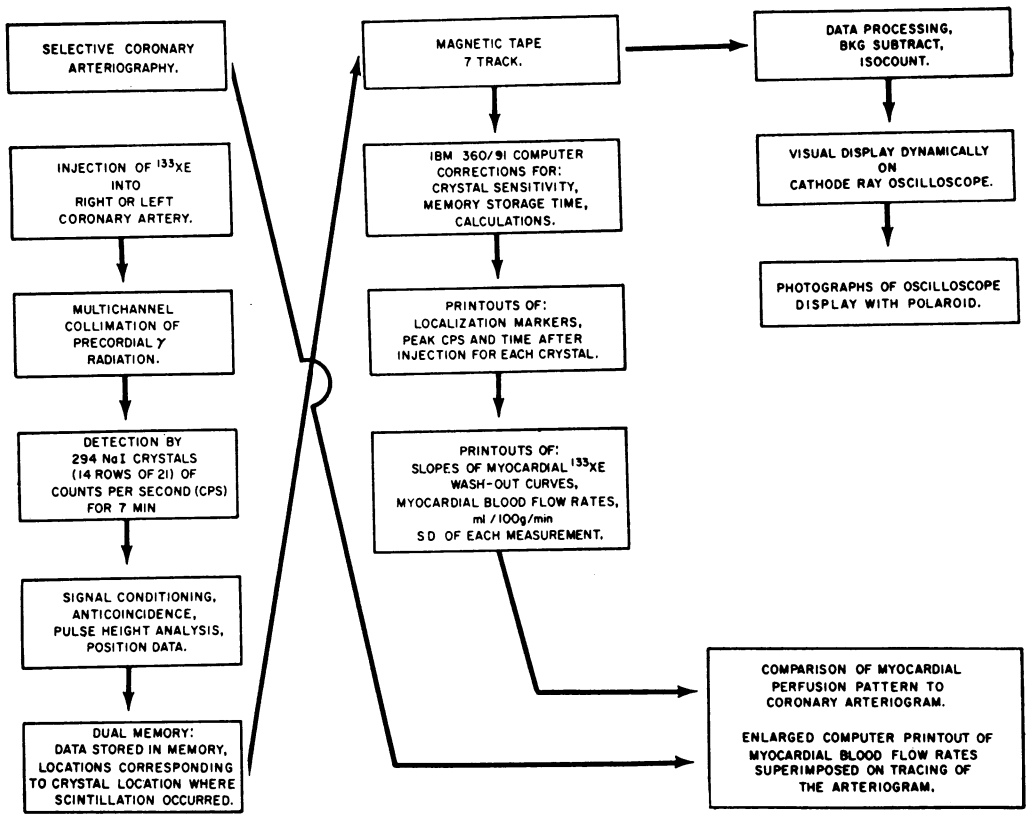

FIGURE 1 Schematic diagram illustrating the sequential steps involved in measurement of regional myocardial blood flow with ^{133}Xe and a multiple-crystal scintillation camera.

areas of the heart instead of attempting to resolve a single multiexponential myocardial wash-out curve as has been done previously (11–16). Data obtained by this new technique in 17 patients with normal coronary arteries are presented.

METHODS

Procedure

A schematic outline of the equipment and sequential procedures involved in the estimation of regional myocardial blood flow is depicted in Fig. 1.

A more detailed consideration of the various steps follows.

Coronary arteriography. Selective coronary arteriography was performed on each subject according to the technique of Sones and Shirey (17). The patient was placed in a supine position on a rotating cradle to obtain films in the right anterior oblique, anterior-posterior, or left anterior oblique projections. Radiopaque isotope markers were placed on the external chest wall in positions indicating the locations of the coronary ostia, upper and lower left or right heart border, and the diaphragmatic surface of the heart. A bolus of 5–10 ml of Renografin-76 contrast material was injected through a No. 8 Sones catheter into the right or left coronary artery; cine films were taken at 64 frames/sec using a 6 inch image intensifier[1] with a 35 mm camera.[2] Upon completion of the arteriogram, 5–10 min were allowed to elapse before measurements of myocardial blood flow were undertaken. During this period, the collimator face of the autofluoroscope (Fig. 2) was positioned over the patient's precordium in the same plane and location where the angiographic camera had previously been situated. The locations of the isotope markers were then recorded by the instrument (*vide infra*) before injection of ^{133}Xe into the coronary artery.

Injection technique. 20–25 mCi of ^{133}Xe dissolved in 1–3 ml of sterile pyrogen-free saline[3] were injected rapidly (2–3 sec) through the catheter into the main right or left coronary artery; this was followed immediately by another 2–4 ml of saline.

Radioactivity detection. The 81 kev γ-radiation emitted by ^{133}Xe in myocardial cells was monitored for 7 min after intracoronary injection by means of the Digital Autofluoroscope (Fig. 2).[4] The autofluoroscope (18) is a scintillation camera in which the radioisotope detecting device consists of a 15 × 23 cm rectangular grid composed of 294 individual NaI(Tl) scintillation crystals arranged in 21 columns of 14 crystals. Each individually shielded crystal (measuring 1.1

[1] North American Phillips, Phillips Medical Systems, Inc., Shelton, Conn.

[2] Arriflex Corp. of America, Woodside, N. Y.

[3] Xenisol, Mallinckrodt Chemical Works, St. Louis, Mo.

[4] Model 5600, Baird Atomic, Inc., Bedford, Mass.

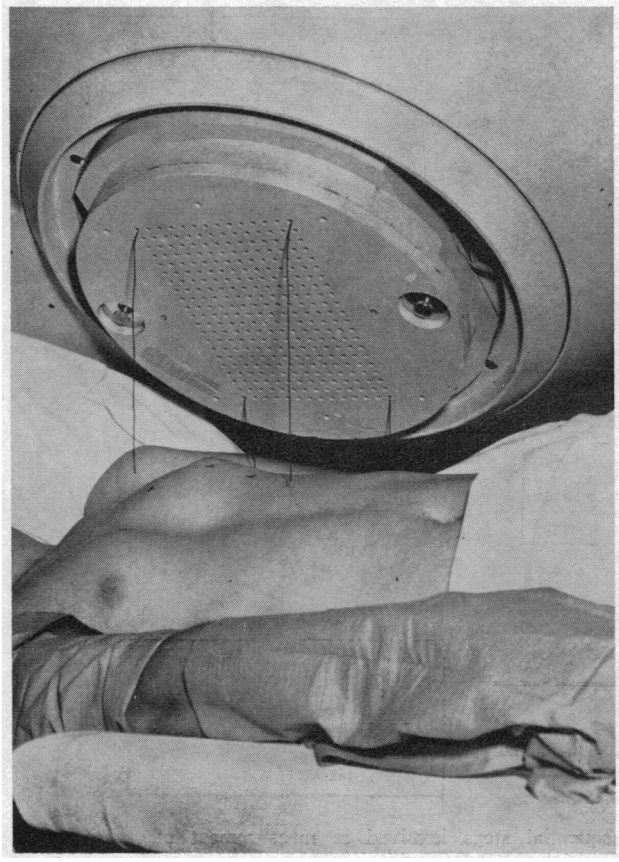

FIGURE 2 Photograph of the Digital Autofluoroscope and the multichannel collimator employed in the studies of regional myocardial blood flow.

$\times$ 1.1 $\times$ 3.5 cm) is optically coupled via light pipes to two of 35 photomultiplier tubes arranged in a 21 $\times$ 14 X and Y coordinate system. Each crystal that scintillates generates pulses in an X and Y phototube, thus precisely defining the location of the crystal. The output of the phototube is electronically amplified and is subjected to pulse height analysis. (Window settings for the present studies were 75–250 kev.) Anticoincidence circuits eliminate pulses arising simultaneously in more than one row or column amplifier due to random coincidence, Compton scatter, or optical cross talk. The pulses leaving the pulse height analyzer are accumulated for a preselected interval (1 sec for the present studies) and are stored in one of two magnetic core memories. At the completion of the preset accumulation time, the data in the core memory are transferred in 45 msec to a magnetic tape for permanent storage.

Machine performance. The performance of each scintillation detector, in the autofluoroscope employed for these studies, was examined by performing seven repetitive countings of a standard ^{57}Co pool. In each test, the distribution of counts recorded by each of the 294 crystals in 23 successive counting intervals was compared with the Poisson distribution by Pearson's chi-square test (19). After initial adjustments of the instrument, 94–96% of the 294 crystals exhibited a Poisson distribution of counts when tested at the 5% significance level in each of seven tests. The 16–18 crystals which did not follow Poisson statistics at this level of significance varied randomly in the different studies.

Using ^{57}Co point sources the total "dead" time resulting from the processing and storage of radioactive impulses was found to be 15 μsec for the autofluoroscope used in the present studies. A "dead" time of this magnitude becomes significant when the peak total count rate recorded by the instrument is 12–30 $\times$ 10^3 cps (the range of peak total myocardial radioactivity observed with the doses of ^{133}Xe used in the present studies). Therefore, the counts from each of the 294 crystals were summed during each counting interval and an appropriate correction based upon a dead time of 15 μsec was applied to the output of each crystal in all calculations of count rate.

Collimation and resolution. The multichannel collimator used in the present studies (Fig. 2) was a lead shield containing one tapered hole for each scintillation crystal location. Because γ-photons pass in straight lines from the source, a radioisotope image is generated by multichannel collimation of γ-emission from an organ source to multiple small detectors; this image has a one-to-one spatial correspondence with the object (Fig. 3).

In contrast to single-crystal scintillation cameras, the intrinsic resolution of the autofluoroscope is energy-independent because it is determined by the geometrical characteristics (10.7 mm^2) of each of the crystals comprising the mosaic pattern of the detector (20). The effective resolution, however, is determined by the thickness of collimator used and the distance from the collimator face to the radioactive source. The relationship between the area viewed by each crystal and the collimator-source distance for the 1.5 inch collimator used in the studies is described by the equation (21) in Fig. 3. The equation probably overestimates the radius of the area viewed by each crystal at any distance, however, because flux across a resolution element is gaussian and is peaked on the axis of the collimator hole (21). With the collimator face resting just on the anterior or anterolateral chest wall, the distances from the chest wall to the anterior and posterior wall of the heart were estimated to be about 4 and 7–8 cm respectively.

Count overlap between adjacent crystals; its effect upon calculations of myocardial blood flow. It is apparent from Fig. 3, that the field of view of one scintillation detector overlaps that of adjacent crystals as the distance of the source from the collimator face increases. In Fig. 4 there appears an estimate of the extent to which overlap of the fields of view of two adjoining crystals (A and B) may influence the slopes of ^{133}Xe washout curves and the calculations of myocardial blood flow in the two adjoining myocardial regions. The experiment depicted in Fig. 5 (top) was performed in order to estimate the magnitude of count-overlap which occurred between crystals at different distances. When results of five similar studies were averaged, (Fig. 5, bottom) the mean overlap of counts between adjacent crystals was 3.0, 3.0, and 16.4% at source to collimator-face distances of 3, 5, and 8 cm respectively.

Oscilloscopic display of data: scintiphotographs. After each study, the radioisotope images produced during ^{133}Xe arrival and washout from various regions of the myocardium were dynamically visualized by replaying the magnetic tape on an oscilloscope. The counts recorded by each crystal were displayed as light of proportional intensity onto a location on the cathode ray tube corresponding to the location of each crystal in the radioactivity detecting device. Scintiphotographs were obtained by photographing the images so generated with a Polaroid camera.

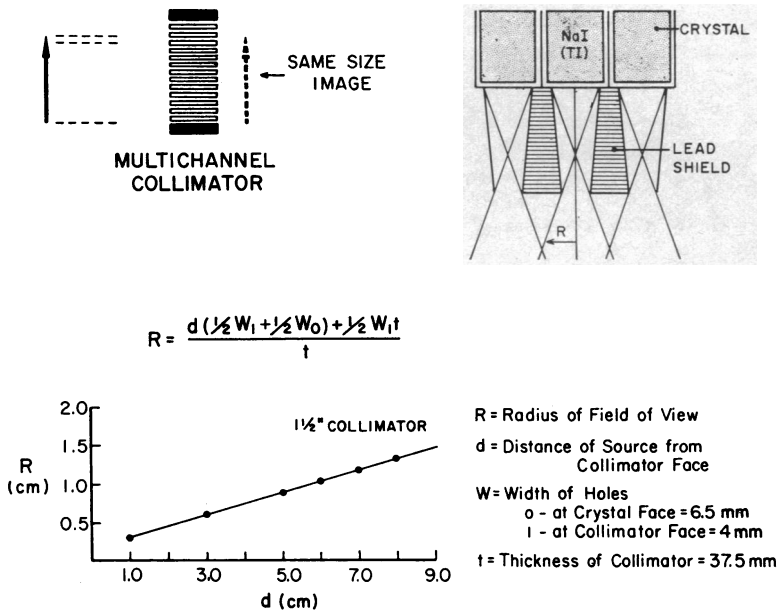

FIGURE 3 Effective resolution of each scintillation detector of the autofluoroscope is determined by the geometry of the channels in the collimator and the distance of the collimator face from the ^{133}Xe source.

Data processing. The magnetic tapes from each study were processed on the IBM 360/91 digital computer at the Columbia University Computer Center. All programs for analysis of the data were written in Fortran IV and will be the subject of another communication. The printout of each frame of information or of derived calculations was arranged in 21 columns of 14 numbers. The position of each number in the printout corresponded to the location in the rectangular grid of the detector of the crystal from which the information was obtained. Six computer printouts were obtained from each study as follows:

Pool count. Before each study, radioactivity from a standard uniform pool of ^{57}Co was measured until the most sensitive crystal had accumulated 1000 counts. A correction factor for each crystal (computed as 1000 counts/recorded counts) was developed in the computer from the pool count to compensate for differences in the relative efficiencies of the different crystals comprising the detector.

Localization. The second printout was of the position of each of the radioactive markers which outlined the cardiac borders.

Counts. The actual cps recorded by each of the 294 crystals during isotope washout from the heart were also printed out in initial studies, so that the ^{133}Xe wash-out curves from various regions could be plotted on semilogarithmic paper for visual and graphical analysis.

Peak cps and time. The computer searched the ^{133}Xe washout curve recorded by each of the 294 crystals and printed out the peak cps as well as the number of seconds after the start of the study that the peak occurred. Table I gives data from the printout of a study of patient H. R. in whom a left coronary artery injection of ^{133}Xe was performed. The peak cps recorded by crystals overlying the myocardium (A-P projection) were higher than peak cps recorded by crystals overlying the lungs. In addition, the highest count rates were observed earlier in crystals above the heart than in crystals above the lung.

Clearance constants of ^{133}Xe washout. Fig. 6 shows two representative semilogarithmic plots of regional (i.e. single-crystal) myocardial ^{133}Xe wash-out curves obtained from one patient who had significant coronary artery disease. In these curves, the initial 1.5-min segments of the isotope disappearance curve were clearly monoexponential. When monitoring was prolonged for 7 min, however, the later portions of the wash-out curves deviated from a single exponential.

The rate constant (k) of a monoexponential equation was calculated by fitting the equation $\ln[\text{cps/peak cps}] = kt$ (using the method of least squares) to the data which were recorded in the first 39 sec after the peak of the curve. An example of the computer printout of the rate constants (k) of 48 myocardial wash-out curves obtained after a single left coronary injection in patient H. W. appears in Fig. 7. Each k is a parameter numerically related to the rate of ^{133}Xe clearance from the myocardial tissue viewed by the individual crystal.

Myocardial blood flow. Myocardial nutrient blood flow in the area viewed by each crystal was estimated by the Schmidt-Kety technique (22-24). The assumptions of this method along with the derivation of the equations which are employed have been reviewed previously (10, 22, 23). Capillary blood flow/100 g of myocardial tissue in each region (F) was calculated by the formula: $F = k \times \lambda/\rho \times 100$ where k is the rate constant of ^{133}Xe washout (determined experimentally), λ is the blood to myocardial tissue partition coefficient for ^{133}Xe which was obtained by Conn in normal dog heart (0.72) (25), and ρ is the specific gravity of the tissue (1.05) (12). A standard deviation of each individual flow measurement (SDM) based upon the scatter of original data points was also calculated for each crystal and included in the computer printout of local myocardial flow rates.

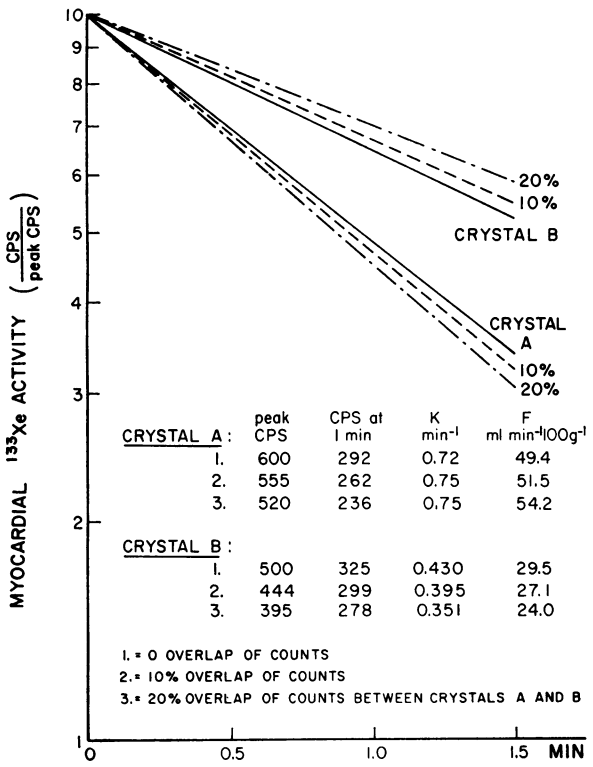

FIGURE 4 Effect of overlap of the fields of view of two adjoining scintillation crystals upon the slopes of ^{133}Xe wash-out curves and the calculations of myocardial blood flow in the two regions. If one assumes that there is no overlap of the fields of view of adjoining crystals, and that the regional myocardial blood flow is 49.4 ml/100 g · min beneath crystal A and is 29.5 ml/100 g · min beneath crystal B, then typical data for the peak cps recorded by each crystal, the cps 60 sec down from the peak of the ^{133}Xe wash-out curve and the slopes of the monoexponential decline of radioactivity and the myocardial blood flow rate in each region appear in lines 1 of the tabulated data. Beneath lines 1 are listed the changes in the original data which would occur if 10% (lines 2) or 20% (lines 3) of the radioactivity beneath crystal A originated from crystal B and vice versa.

Comparison of coronary arteriogram with the myocardial perfusion pattern. The schematic diagram in Fig. 8 is a composite made from the chest X-ray, atrioventriculogram, and coronary arteriogram of a single patient; it illustrates in the A-P projection the positions of the four cardiac chambers relative to the cardiac silhouette and to the right and left coronary arteries. Because the mosaic of scintillation crystals employed to measure myocardial perfusion in these studies detects precordial radioactivity from a 23 × 15 cm area, it it apparent that the individual detectors measure ^{133}Xe washout from various regions of the cardiac anatomy.

Upon completion of the arteriography and flow studies, the arteriograms were displayed on white paper with a 2.4-fold magnification of cardiac distances, and a tracing of each coronary vessel with its major branches was made (only arteriograms in which third order coronary vessels could be clearly visualized were included in the studies.) The computer printout of local myocardial perfusion rates was similarly enlarged and superimposed onto the tracing of the arteriogram so that the radiopaque markers on the X-ray coincided with the radioactive markers observed on the computer printout.

Statistical analysis. Results were analyzed by standard statistical techniques (26). Changes were termed significant if P was < 0.05 unless otherwise specified in the text.

RESULTS

Patterns of regional myocardial perfusion. The four scintiphotographs in Fig. 9 show the radioisotope images produced by ^{133}Xe in myocardial tissue 1, 3, 5, and 128 sec after injection into a main left coronary artery. They depict not only the size of the area perfused by the left coronary artery but also the extremely rapid diffusion of the inert gas out of coronary vessels into the myocardial tissue. Fig. 10 shows a tracing of the same pa-

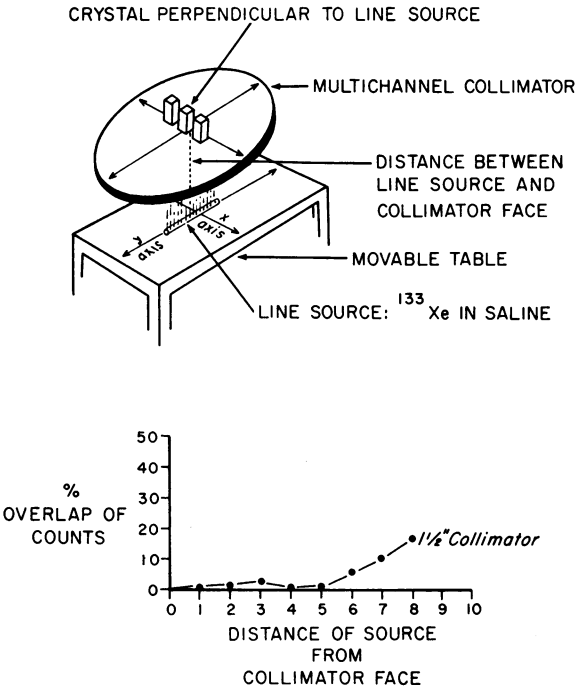

FIGURE 5 A capillary tube (1 mm diameter) containing ^{133}Xe dissolved in saline was positioned parallel to the collimator face at a distance of 1 cm; the line source was centered beneath and oriented along the y axis of the collimator hole of a single scintillation crystal (top of figure). While 200–500 counts were being accumulated by the crystal which was directly perpendicular to the radioactive source, the number of counts simultaneously detected by the two adjacent scintillation crystals (on the x axis of the primary crystal) were measured and recorded. Subsequently the distance between the source and the collimator was progressively increased by 1 cm increments and the radioactivity measurements by the three crystals were repeated at each distance. At the bottom of the figure the mean of counts recorded by the two adjacent crystals is represented as a percentage of the counts recorded by the crystal overlying the source and is plotted as a function of the distance of the source from the collimator face.

tient's coronary arteriogram superimposed onto the computer printout of local myocardial blood flow rates in ml/100 g·min. Apparent in this patient with a radiographically normal left coronary artery is a small inhomogeneity of local nutrient blood flow rates in the left ventricular myocardium. Mild inhomogeneity of left ventricular myocardial perfusion rates is also apparent in two sequential studies of another patient with a normal left coronary artery (Fig. 11 *a* and 11 *b*). Lower myocardial flow rates were recorded by crystals in the upper left of this pattern, possibly because the left ventricle and left atrium are superimposed in this region (Fig. 8).

The duplications of regional myocardial perfusion rates found in sequential studies 11 *a* and *b* are representative of the reproducibility of the method. Five pairs of sequential studies were subjected to analysis of variance by the computer. The variance of differences in perfusion between individual crystals on repeat studies was not significantly different from the variance of differences in

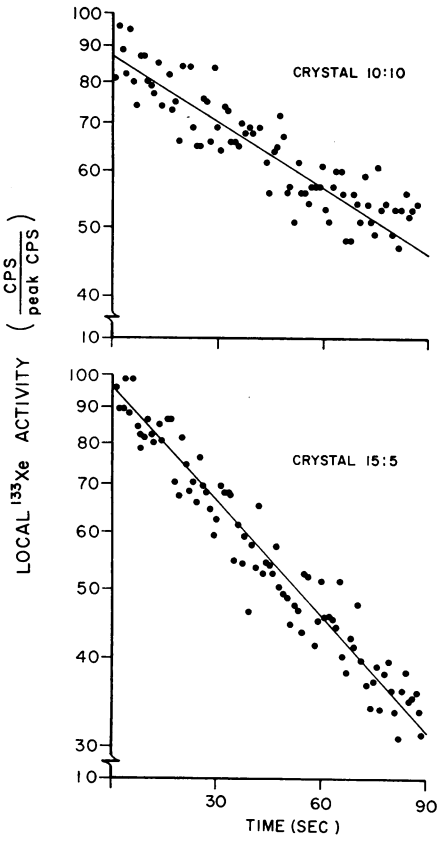

FIGURE 6 Two semilogarithmic plots of myocardial ^{133}Xe activity (cps/peak cps against time) are depicted. These were obtained by two crystals in one patient. The patient had coronary artery disease; one crystal overlay myocardium supplied by a normal vessel (bottom); the other (top) was over tissue supplied by a narrowed branch of the left coronary.

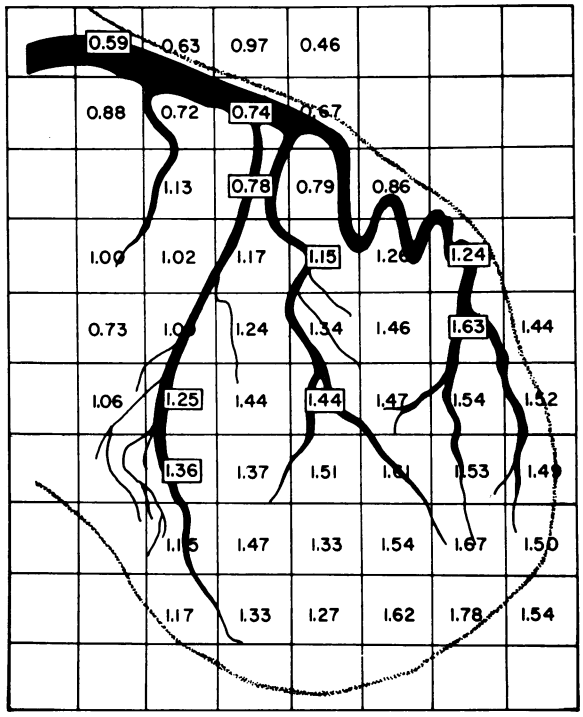

FIGURE 7 A computer printout of the slopes of the 48 myocardial ^{133}Xe wash-out curves obtained after a single left coronary injection in patient H. W. is shown (A-P projection).

mean ventricular flow rates or in the flow rates found in left ventricular regions supplied by the three principle branches of the left coronary artery.

Scintiphotographs obtained after injection of ^{133}Xe into a dominant normal right coronary artery are shown in Fig. 12; (patient A. S., LAO position) a C-shaped radioisotope image was produced on the oscilloscope as ^{133}Xe passed from the capillary distribution of the vessel into tissue of the right atrium, right ventricle, and apical-inferior portions of the left ventricle. Fig. 13, shows a tracing of the arteriogram superimposed upon the pattern of myocardial perfusion rates obtained in this study. Tissue perfusion was lower in the right atrial region than in the right ventricular region; tissue perfusion was highest in the left ventricular tissue supplied by this artery.

Myocardial blood flow rates in left and right ventricle. In each of 17 patients with normal coronary arteries, the myocardial perfusion rates recorded by crystals overlying the right atrium, the right ventricle, and the left ventricle have been averaged to obtain a mean myocardial blood flow rate for each region of the heart; the data are plotted in Fig. 14. In this group, with clinical and hemodynamic evidence of heart disease (27) but normal coronary arteriograms, the average myocardial blood flow

TABLE I

Printout of Peak cps and Time

59	58	197	83	158	118	205	189	152	181	183	137
179	147	172	142	178	176	178	149	150	173	5	172
54	79	156	81	166	105	123	219	114	182	213	132
131	162	149	125	122	134	130	5	5	5	6	5
99	82	167	80	126	155	396	488	327	261	274	106
169	162	165	149	152	117	5	5	5	5	5	107
83	111	150	100	242	399	461	661	615	447	229	108
171	179	121	140	7	5	5	5	5	5	5	94
133	124	149	125	515	461	496	374	355	294	189	116
151	144	150	114	7	7	7	5	5	5	5	95
158	113	172	241	623	447	358	377	173	148	160	117
157	139	128	7	7	7	10	7	7	113	111	89
124	138	292	416	742	325	409	371	112	151	130	109
118	126	14	8	7	7	7	8	64	77	111	72
157	134	442	457	678	318	622	310	113	151	147	146
117	152	13	9	7	8	8	11	68	107	65	81
110	147	329	298	422	272	295	181	113	150	150	108
107	81	9	8	8	8	9	71	108	76	82	85
137	130	401	376	458	249	331	212	132	181	155	123
75	110	9	8	8	9	10	88	71	67	86	63
114	106	304	296	394	218	212	215	127	120	121	100
125	117	9	8	16	11	60	85	56	78	81	68
109	89	117	140	108	117	179	190	107	109	104	106
125	141	154	70	109	88	69	65	66	65	60	94

A portion of the computer output depicting the peak cps recorded by each crystal (top number) and the number of seconds after the start of the study when peak cps occurred in each crystal is presented. The peak cps were higher and occurred sooner in crystals overlying myocardium than in those overlying the lungs.

rate in the left ventricle, 64.1 ±13.9 ml/100 g·min, significantly exceeded that in the right ventricle, 47.8 ±10.9 ml/100 g·min, and that in the right atrium, 33.6 ±10.3 ml/100 g·min.

DISCUSSION

The present method of measuring regional myocardial blood flow in man using ^{133}Xe and a multiple-crystal scintillation camera is another adaptation of the inert gas clearance technique to measure tissue perfusion (22–24). While similar in principle to other measurements of myocardial flow using inert gases, nevertheless, it differs in several respects.

Previous investigators have: (*a*) monitored either the single washout curve of an inert gas injected into a coronary artery (11, 14, 16, 28) or the myocardial extraction of an isotopic indicator (29, 30), or (*b*) they have measured the washout rates of an inert gas which was injected directly into various regions of the myocardium with a needle (31, 32). Although the former techniques provided information about blood flow/gram over a large area of the heart (a ventricle or more), they proved unsatisfactory in study of patients with coronary artery disease. This inadequacy resulted because local areas of reduced perfusion were obscured by the higher flow in normally perfused regions and because hetero-

geneous myocardial flow in coronary patients caused the single inert gas wash-out curves obtained by these methods to deviate from a single exponential equation in a fashion that could not be resolved mathematically (16). The technique of sequential measurements of local inert gas clearance after direct injections (32) is limited by need for a thoracotomy and by tissue effects caused by the needle. More recently, radioactive microspheres have been used to demonstrate regional myocardial flow variations in experimental animals (33, 34). As recently adapted to studies of man, (35), however, the microsphere technique does not give quantitative myocardial blood flow data.

In the present method, the myocardial tissue supplied by the coronary artery into which the ^{133}Xe is injected is subdivided into a relatively large number of small regions by means of a multichannel collimator and multiple miniature scintillation detectors. The wash-out curves are monitored simultaneously from the different regions, and the rate constants (k) of isotope removal are calculated by computer monoexponential analysis of the initial 39 sec of each curve. Each parameter (k) is a quantitative expression of the capacity of the local circulation in each of the multiple cardiac regions to eliminate a diffusible substance (and by inference to supply the tissue with diffusible nutrients). Each is directly related to the local capillary blood flow by the ratio λ/ρ (23, 24). In order to express the primary data in terms of blood flow, regional myocardial perfusion rates are calculated by the Kety formula (12, 23, 24) using an assumed value for λ. The resulting regional myocardial perfusion patterns are then compared with the patient's coronary arteriogram which was taken during the same study.

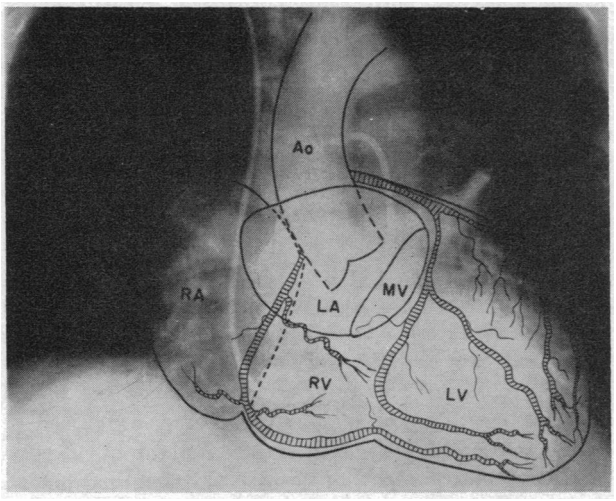

FIGURE 8 This composite made from the chest X-ray, atrioventriculogram, and coronary arteriogram of a single patient illustrates the relative positions of the cardiac chambers and coronary arteries in A-P projection. LV, left ventricle; RV, right ventricle; LA, left atrium; RA, right atrium; MV, mitral valve; Ao, aorta.

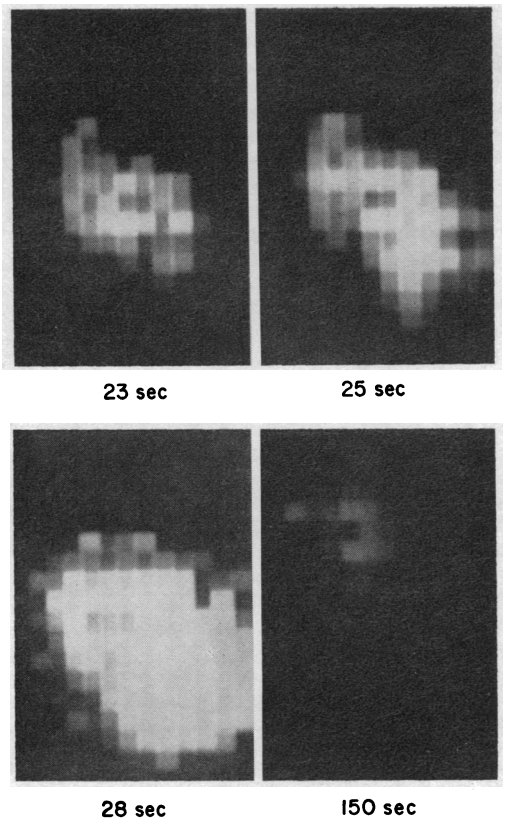

FIGURE 9 The four scintiphotographs shown in the figure are 1 sec integrated Polaroid photographs of the cathode-ray oscilloscope of the autofluoroscope. They were obtained during replay of the magnetic tape of the study of patient H. W. in which ^{133}Xe was injected into the left coronary artery. The pictures show isotope location in the myocardium, 1, 3, 5, and 128 sec after injection which was made at second 22.

Three arbitrary selections were made in the present studies and deserve comment: (*1*) ^{133}Xe as indicator, (*2*) the monoexponential analysis of the data, and (*3*) use of 0.72 as the blood: myocardium partition coefficient for Xenon. Other choices might conceivably have been made without invalidating the approach.

(*1*) ^{133}Xe was used as the isotopic indicator because the diffusibility of ^{133}Xe is not limited by capillary pore size (10, 23, 24). The low energy γ-emission of this isotope can be detected externally but does not penetrate septae in the multichannel collimator, a feature which enhances resolution. The combination of low energy emission plus a short biological half-life due to rapid pulmonary elimination (14, 36) also limits radiation ex-

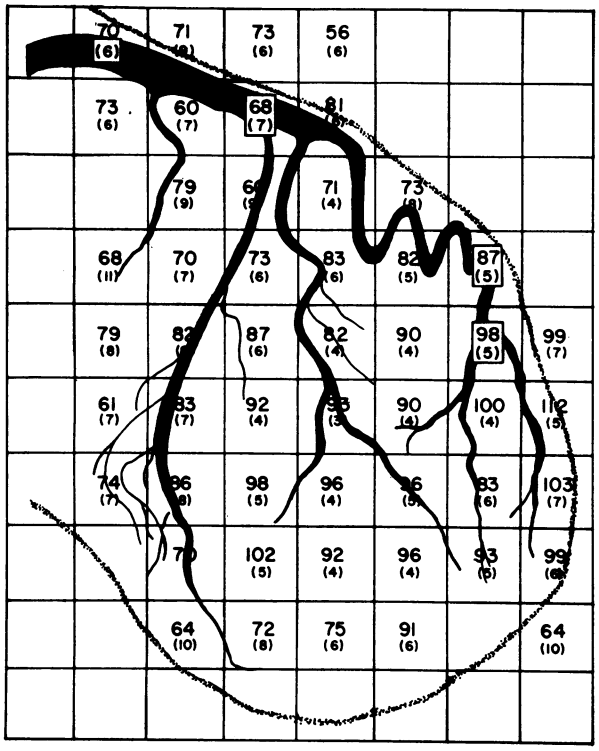

FIGURE 10 This is the computer printout showing the myocardial blood flow rates (ml/100 g · min) in different regions of the heart. The blood flow rates were calculated from the multiple ^{133}Xe wash-out curves obtained after ^{133}Xe injection into the left coronary artery of H. W. The printout has been magnified, aligned, and superimposed upon a tracing of the coronary arteriogram of H. W. which was obtained during the same study. The areas recorded by each of the crystals are indicated by the rectangles. The standard deviation of each flow measurement (ml/100 g · min) appears in brackets below each value for regional myocardial blood flow.

posure to the patient. An intravenous or intra-arterial injection of 40 mCi of ^{133}Xe dissolved in saline yields a gonadal dose of 10 mrads (2% of the gonadal dose from an ordinary flat plate of the abdomen), a level considered safe for routine diagnostic isotope work (37).

(2) A monoexponential analysis of the initial 39 sec after the peak cps of each ^{133}Xe wash-out curve was performed. This form of analysis was chosen for several reasons: (*a*) The initial portions of the curves were clearly linear when plotted semilogarithmically against time (Fig. 6). (*b*) In three reported studies using flow meters in experimental animals, there was a close correspondence between directly measured coronary artery flow/gram tissue and myocardial blood flow rates calculated from the initial segment of ^{133}Xe or ^{85}Kr myocardial wash-out curves (12, 14, 15). (*c*) The slope of the initial most rapid portion of the curve is probably least effected by the content of nonmuscular tissue (e.g., fat) in the field of view monitored by each crystal (15).

Height/area analysis was not performed in the present studies because there is uncertainty where to terminate such an analysis (38, 39). Furthermore, additional studies with the scintillation camera, in which the time-course of ^{133}Xe appearance in lung tissue beside or behind the heart was monitored after tracer injection into a coronary artery or the right atrium, revealed that only small amounts of radioactivity were present in lung tissue behind the heart during the first 40 sec of myocardial washout. It is conceivable that the more significant buildup of intrapulmonary counts which occurred later (Table I) might distort a height/area analysis. A two compartment analysis of the curves was not selected, because this type of analysis grossly underestimated the directly measured myocardial flow/gram in a study (15) in which a two compartment model was tested by comparison with a flow meter in dog hearts.[5]

(3) In order to express the measurements of isotope washout in physiological terms of nutrient blood flow/100 g·min, each of the rate constants obtained experimentally has been multiplied by a factor (68.6) which is based upon an untested assumption that in each of the myocardial regions λ is 0.72, a value similar to that obtained in static studies of normal canine myocardium (25). Canine myocardium contains relatively little fat. The theoretical possibility that ^{133}Xe wash-out curves might be altered in different regions of the human heart because of changes in the local λ due to differing concentrations of muscle, fat, and other tissue components exists, but has not been approached experimentally. Other investigators have shown, however: (*a*) that diffusion equilibrium for ^{133}Xe between myocardial tissue and fat is not complete 30 sec after intracoronary injection of isotope (15), and (*b*) that persistance of isotope in cardiac fat influences the tail of ^{133}Xe washout curves to a much greater extent than it influences the more rapidly changing initial portions of the curve (15, 40). Therefore only data points recorded during the first 39 sec after the peak of the ^{133}Xe wash-out curves were analyzed in the present studies in order to minimize possible effects of fat or other nonmuscular components of myocardium on the blood flow calculations.

The problem of how to determine the in vivo λ for an inert gas in different regions of a tissue comprised of heterogeneous elements is currently not solved. Experimental verification of λ in normal and abnormal human myocardial tissue is required. Alternatively, this un-

[5] A monoexponential approach was not endorsed in this careful study in which different forms of analysis of single myocardial wash-out curves were compared. Nevertheless, the data of these investigators ([15] Table II) show that, of the common methods of analysis, the monoexponential came the closest to the actual measured flow.

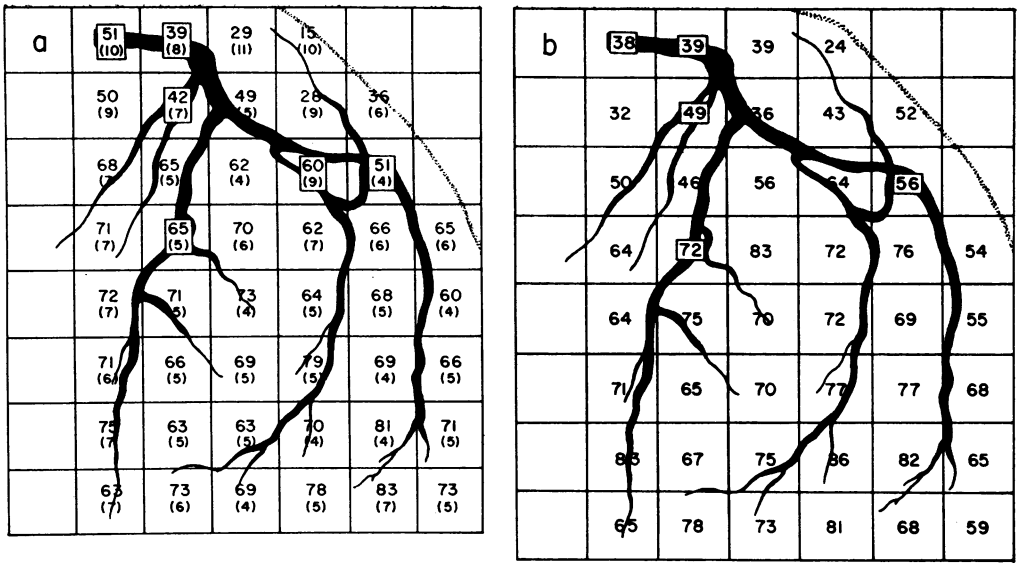

FIGURE 11*a* and *b* In the figure, two successive studies of left ventricular myocardial perfusion rates in patient H. P. are depicted. Each myocardial perfusion pattern has been superimposed upon a tracing of the patient's coronary arteriogram.

certainty could perhaps be avoided by use of an isotopic indicator which is not fat soluble (41) such as water labeled with oxygen-15.

In summary therefore, the primary results in the present studies are the slopes (k) of the multiple ^{133}Xe myocardial wash-out curves. The regional myocardial perfusion rates calculated from the primary data must be interpreted with a degree of caution to the extent that the numerical results depend upon assumptions inherent in a monoexponential analysis of the isotope washout curves, and to the extent that the expression of the results in terms of nutrient blood flow depends upon an assumed constant, λ. The basic experimental approach and observations, (i.e., simultaneous multiple measurements of isotope washout from multiple regions of the heart with a scintillation camera) retains a validity, however, which

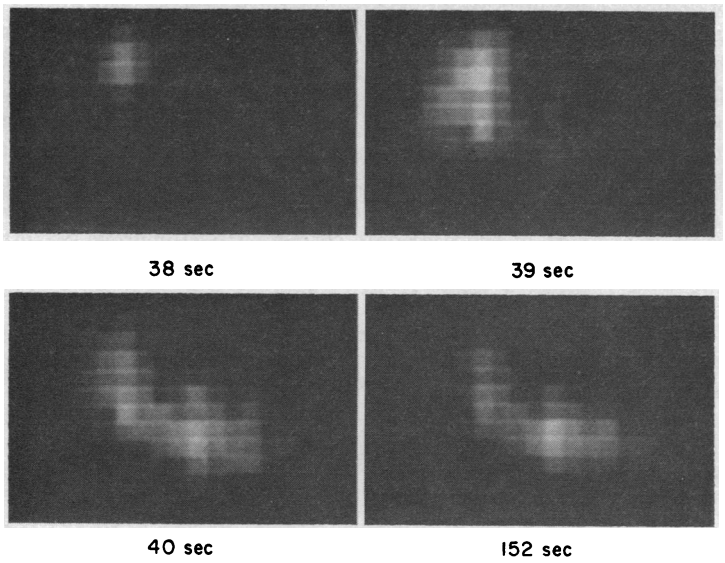

FIGURE 12 Sequential scintiphotographs taken after ^{133}Xe injection into a dominant normal right coronary artery of patient A. S. are shown. A C-shaped radioisotope image was produced.

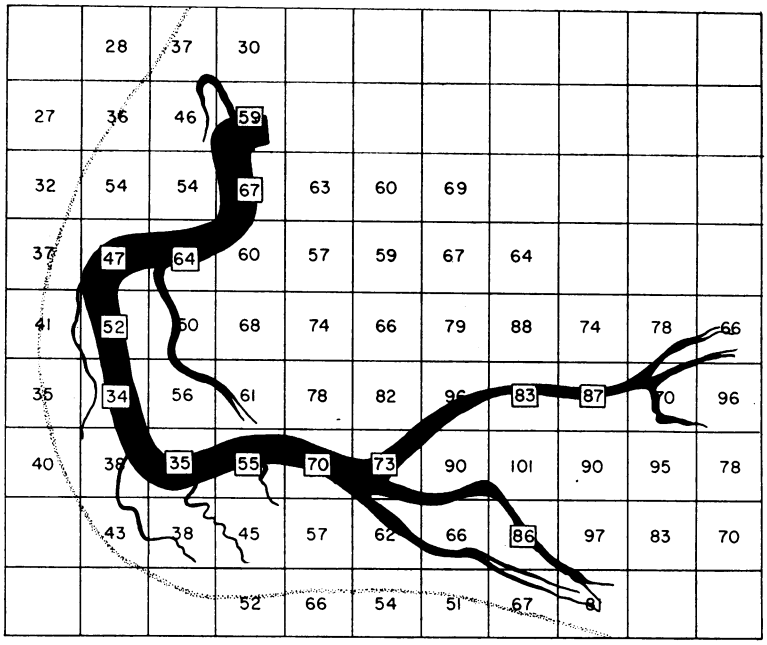

FIGURE 13 The computer printout showing myocardial blood flow/100 g · min by each crystal has been superimposed upon a tracing of the right coronary arteriogram. Myocardial perfusion rates were lower in crystals to the left of the right coronary artery proximal to the acute margin (right atrial region) than in those to the right of the main right coronary (right ventricle); they were highest in crystals along the posterior descending branch (inferior left ventricle).

is independent of a form of mathematical analysis and of the assumptions involved in expressing the data in units of flow.

The new method to estimate regional myocardial perfusion has several advantages. The study may be performed in intact subjects at the time of coronary arteriography with no additional risk to the patient other than the slight radiation exposure due to isotope injection. Because ^{133}Xe is delivered to the myocardium via a coronary artery, local tissue hyperemia due to a direct needle injection of indicator is avoided. Since most of the ^{133}Xe washed out of cardiac tissue is excreted in one passage by the lungs (14, 36), recirculation of the remainder is so minimal that isotope does not appear in the chest wall in sufficient amounts to alter myocardial wash-out curves.[6] The scintillation camera allows quantitative measurements of isotope removal from many areas of the myocardium to be carried out simultaneously.[7] Replay of the data tape on an oscilloscope also provides visual representations of isotope location in the myocardium which are proportional in size and shape to the tissue bed supplied by the artery which was injected.

Most of the limitations of the present method in its current stage of development, in addition to the high cost of the equipment and isotope, relate to the states of the technology involved. Technological improvements in design of the scintillation camera might: (*a*) reduce "dead" time which currently necessitates a computer correction; (*b*) improve the instrument's intrinsic resolution (1.1 cm), and (*c*) increase the efficiency of counting.

The other limitations to this new approach relate to the facts: (*a*) that the ^{133}Xe wash-out rate recorded by an individual crystal represents removal of isotope from all myocardial tissue within its field of view, and (*b*) that the heart is spherical. For the former reason differences between endocardial and epicardial flows have not been

[6] In the studies to date, spillage of isotope into the aorta with obscuration of myocardial washout of ^{133}Xe by accumulation of the tracer in overlying chest wall has not been a problem for two reasons: (*a*) Isotope movement down the aorta can be detected during replay of the magnetic tape on the oscilloscope. (*b*) Dilution of ^{133}Xe (10 mCi) injected into the root of the aorta by aortic blood flow was so great that the count rates recorded by crystals overlying the chest wall were not significantly increased above background.

[7] It is quite possible that data similar to that obtained by a multiple crystal scintillation camera could be obtained with a single-crystal scintillation camera combined with computer crystal-splitting techniques. Relative merits of the two types of instrument, however, would depend upon collimation, the degree of count overlap between adjacent areas and the precision of measurement in each region.

detected. Because of the spherical cardiac shape two or more myocardial surfaces supplied by one artery are viewed by the same scintillation crystal in certain areas of the heart (Fig. 8). If, in the future, collimation and crystal sensitivity can be improved, it may be possible to make several injections of ^{133}Xe and regional myocardial flow measurements from multiple views in the same patient.

Despite the limitations, the present studies indicate that in patients with heart disease but arteriographically normal coronary arteries (Figs. 10–14) there are considerable variations in the myocardial blood flow rates in different regions of the human heart, despite a relative homogeneity of local perfusion rates in a given area (e.g., left or right ventricle). These differences in regional perfusion rates in patients with radiographically normal coronary arteries may explain, in part, the deviations from a single exponential observed in the past when a single inert gas wash-out curve from a large area of normal myocardium was plotted semilogarithmically against time (11–14, 16, 28). In other studies (27), areas of reduced myocardial perfusion have been detected and localized to specific vascular lesions in patients with coronary artery disease.

The results obtained in 17 patients with radiographically normal coronary arteries indicate that the mean rate of washout of ^{133}Xe from left ventricular myocardium is significantly faster than from right ventricular myocardium or the right atrial region. These findings confirm previous observations of Pitt, Friesinger, and Ross (42) who monitored ^{133}Xe wash-out curves with a single precordial detector. The results differ from those of Klein, Cohen, and Gorlin (28) who found no differences between left and right coronary flow in nine subjects using ^{85}Kr, coronary sinus sampling and a two compartment analysis of the wash-out curves.

The possibility that right ventricular or basal epicardial fat retarded isotope washout and spuriously reduced the calculated right heart perfusion rates cannot be completely excluded in the present study. Precautions taken to obviate this possibility have been discussed previously. However, it may be noted that left ventricular myocardial perfusion has exceeded that of the right ventricle in experimental animals in several studies in which the myocardial blood flow measurements were made with Rb^{86} or radioactive microspheres (29, 33, 43), two different techniques which are not influenced by the fatty content of the tissue. Since myocardial oxyen consumption, a major factor influencing coronary blood flow, is largely determined by pressure generation in the ventricle (44, 45) the finding of greater perfusion per gram myocardium in left ventricle compared with right ventricle in patients with radiographically normal coronary arteries suggests that the greater pressure work of the left ventricle requires not only a greater muscle mass, but also a larger blood supply per unit tissue than in the right ventricle.

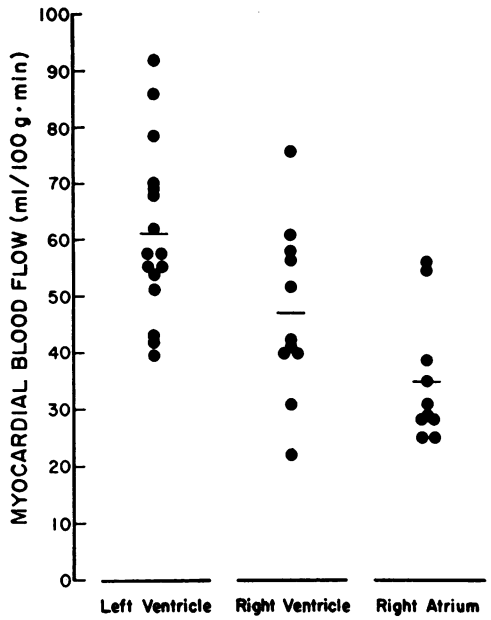

FIGURE 14 In each of 17 patients with normal coronary arteries, the perfusion rates obtained by crystals overlying left ventricle, right ventricle and right atrial region were averaged, the mean value obtained is plotted on the graph. The average left ventricular capillary blood flow rate exceeded that in the right ventricle and that in the right atrial region.

The present approach to the quantitative assessment of regional myocardial perfusion in man with ^{133}Xe and a scintillation camera would appear to have several immediate clinical applications if used together with selective coronary arteriography: (*a*) localization of ischemic or functionally avascular areas of the myocardium; (*b*) assessment of the effectiveness of the collateral circulation to regions beyond coronary arterial occlusive lesions; (*c*) study of diseases which affect the coronary microcirculation; (*d*) pharmacological investigation of drug influences in ischemic regions of the heart; and (*e*) critical evaluations of surgical procedures proposed to revascularize the myocardium.

ACKNOWLEDGMENTS

We would like to acknowledge the able technical assistance of Miss Jean Webster and to thank Miss Lee Nussdorf for the computer programming and data processing.

This work was supported by grants HE 10182, HE 05741. HE 14148, HE 14236, and 5 R01 HD 03993 from the U. S. Public Health Service.

REFERENCES

1. Brener, B. J., A. B. Warren, and R. Warren. 1965. Internal mammary implantation operation for relief of myocardial ischemia. *N. Engl. J. Med.* **273**: 479.
2. Dilley, R. B., J. A. Cannon, A. A. Kattus, R. N. McAlpin, and W. P. Longmire, Jr. 1965. The treatment of coronary occlusive disease by endarterectomy. *J. Thorac. Cardiovasc. Surg.* **50**: 511.
3. Green, G. E., S. H. Stertzer, and E. H. Reppert. 1968. Coronary arterial bypass grafts. *Ann. Thorac. Surg.* **5**: 443.
4. Lillehei, C. W., A. J. Lande, W. R. Rassman, S. Tanaka, and J. H. Bloch. 1969. Surgical management of myocardial infarction. *Circulation.* **1**(Suppl. IV): 35.
5. Alfonso, S., G. G. Rowe, W. C. Lowe, and C. W. Crumpton. 1963. Systemic and coronary hemodynamic effects of isosorbide dinitrate. *Amer. J. Med. Sci.* **246**: 584.
6. Grant, R. H. E., P. Keelan, R. J. Kernohan, J. C. Leonard, L. Nancekieville, and K. Sinclair. 1966. Multicenter trial of propranalol in angina pectoris. *Amer. J. Cardiol.* **18**: 361.
7. Killip, T. III, and J. T. Kimball. 1967. Treatment of myocardial infarction in a coronary care unit: a two year experience with 250 patients. *Amer. J. Cardiol.* **20**: 457.
8. Vital Statistics in the United States 1967. 1969. R. H. Finch, Secretary, W. H. Stewart, Surgeon General. U. S. Department of Health, Education and Welfare. Public Health Service, Washington, D. C. 1.
9. Proudfit, W. L., E. K. Shirey, and F. M. Sones, Jr. 1966. Selective cine coronary arteriography: correlation with clinical findings in 1000 patients. *Circulation.* **33**: 901.
10. Cannon, P. J., J. I. Haft, and P. M. Johnson. 1969. Visual assessment of regional myocardial perfusion utilizing radioactive Xenon and scintillation photography. *Circulation.* **40**: 277.
11. Eckenhoff, J. E., J. H. Hafkenschiel, M. H. Harmel, W. T. Goodale, M. Lubin, R. J. Bing, and S. S. Kety. 1948. Measurement of coronary blood flow by the nitrous oxide method. *Amer. J. Physiol.* **152**: 356.
12. Herd, J. A., M. Hollenberg, G. D. Thorburn, H. H. Kopald, and A. C. Barger. 1962. Myocardial blood flow determined with Krypton 85 in unanesthetized dogs. *Amer. J. Physiol.* **203**: 122.
13. Cohen, L. S., W. C. Elliott, and R. Gorlin. 1964. Measurement of myocardial blood flow using krypton 85. *Amer. J. Physiol.* **206**: 997.
14. Ross, R. S., K. Ueda, P. R. Lichtlen, and J. R. Rees. 1964. Measurement of myocardial blood flow in animals and man by selective injection of radioactive inert gas into the coronary arteries. *Circ. Res.* **15**: 28.
15. Bassingthwaighte, J. B., T. Strandell, and D. E. Donald. 1968. Estimation of coronary blood flow by washout of diffusible indicators. *Circ. Res.* **23**: 259.
16. Klocke, F. J., R. C. Koberstein, D. E. Pittman, I. L. Bunnell, D. G. Greene, and D. R. Rosing. 1968. Effects of heterogeneous myocardial perfusion on coronary venous H_2 desaturation curves and calculations of coronary flow. *J. Clin. Invest.* **47**: 2711.
17. Sones, F. M., Jr., and E. K. Shirey. 1962. Cine coronary anteriography. *Mod. Concepts Cardiovasc. Dis.* **31**: 735.
18. Bender, M. A. 1966. Recent advances in nuclear medicine. Croll and Brady, editors. Appleton-Century Crofts, New York. 1.
19. Matthinsen, C., and J. W. Goldzieher. 1965. Precision and reliability in liquid scintillation counting. *Anal. Biochem.* **10**: 401.
20. Lorenz, W. J., P. Schmidlin, H. Kampmann, H. Ostertag, W. E. Adam, H. Arnold, and W. Maier-Borst. 1968. Comparative investigations with the Anger scintillation camera and the digital autofluoroscope. Symposium on Medical Radioisotope Scintography. International Atomic Energy Agency, Salzburg, Austria.
21. Grenier, R., and J. V. DiRocco. 1968. Performance characteristics of the digital autofluoroscope. *IEEE Trans. Nucl. Sci.* **15**: 366.
22. Kety, S. S. 1949. Measurement of regional circulation by the local clearance of radioactive sodium. *Amer. Heart J.* **38**: 321.
23. Kety, S. S. 1951. Theory and applications of exchange of inert gas at lungs and tissues. *Pharmacol. Rev.* **3**: 1.
24. Kety, S. S. 1960. I. Blood-tissue exchange methods. Theory of blood-tissue exchange and its application to measurement of blood flow. *Methods Med. Res.* **8**: 223.
25. Conn, H. L., Jr. 1961. Equilibrium distribution of radioxenon in tissue: Xenon-hemoglobin association curve. *J. Appl. Physiol.* **16**: 1065.
26. Dixon, W. J., and F. J. Massey, Jr. 1957. Introduction to Statistical Analysis. McGraw-Hill, Inc., New York. 232.
27. Cannon, P. J., R. B. Dell, and E. M. Dwyer, Jr. 1972. Regional myocardial perfusion rates in patients with coronary artery disease. *J. Clin. Invest.* **51**: 978.
28. Klein, M. D., L. S. Cohen, and R. Gorlin. 1965. Krypton 85 myocardial blood flow: precordial scintillation versus coronary sinus sampling. *Amer. J. Physiol.* **209**: 705.
29. Love, W. D., and G. E. Burch. 1957. A study in dogs of methods suitable for estimating the rate of myocardial uptake of Rb^{86} in man and the effect of l-norepinephrine and pitressin on Rb^{86} uptake. *J. Clin. Invest.* **36**: 468.
30. Cohen, A., E. J. Zaleski, H. Baleiron, T. B. Stock, C. Chiba, and R. J. Bing. 1967. Measurement of coronary blood flow using Rubidium^{84} and the coincidence counting method—a critical analysis. *Amer. J. Cardiol.* **19**: 556.
31. Hollander, W., I. M. Madoff, and A. V. Chobanian. 1963. Local myocardial blood flow as indicated by the disappearance of NaI^{131} from heart muscle: studies at rest, during exercise and following nitrite administration. *J. Pharmacol. Exp. Ther.* **139**: 53.
32. Sullivan, J. M., W. J. Taylor, W. C. Elliott, and R. Gorlin. 1967. Regional myocardial blood flow. *J. Clin. Invest.* **46**: 1402.
33. Domenech, R. J., J. I. E. Hoffman, M. I. M. Noble, K. B. Saunders, J. R. Hensen, and S. Subijanto. 1969. Total and regional coronary blood flow measured by radioactive microspheres in conscious and anesthetized dogs. *Circ. Res.* **25**: 581.
34. Becker, L. C., N. J. Fortuin, and B. Pitt. 1971. Effect of ischemia and antianginal drugs on the distribution of radioactive microspheres in the canine left ventricle. *Circ. Res.* **28**: 263.
35. Ashburn, W. L., E. Braunwald, A. L. Simon, and J. H. Gault. 1970. Myocardial scanning in man using Technetium-99 m macroaggregated albumins. *Circulation.* **42** (Suppl. 3): 95.
36. Chidsey, C. A. III, H. W. Fritts, Jr., A. Hardewig, D. W. Richards, and A Cournand. 1959. Fate of radioactive Krypton (Kr^{85}) introduced intravenously in man. *J. Appl. Physiol.* **14**: 63.

37. Lassen, N. A. 1964. Assessment of tissue radiation dose in clinical use of radioactive inert gases with examples of absorbed doses from 3-H, 83-Kr, 133-Xe. *Minerva Nucl.* **8**: 211.
38. Zierler, K. L. 1965. Equations for measuring blood flow by external monitoring of radioisotopes. *Circ. Res.* **16**: 309.
39. Bassingthwaighte, J. B. 1970. Blood flow and diffusion through mammalian organs. *Science (Washington).* **167**: 1347.
40. Shaw, D., G. C. Friesinger, A. Pitt, and R. S. Ross. 1966. Macro-autoradiography of Xenon 133 in the myocardium. *Fed. Proc.* **25**: 401.
41. Ter-Pogossian, M. M., J. O. Eichling, D. O. Davis, and M. J. Welch. 1970. The measure in vivo of regional cerebral oxygen utilization by means of oxyhemoglobin labeled with radioactive oxygen-15. *J. Clin. Invest.* **49**: 381.
42. Pitt, A., G. C. Friesinger, and R. S. Ross. 1969. Measurement of blood flow in the right and left coronary artery beds in humans and dogs using the ^{133}Xenon technique. *Cardiovasc. Res.* **3**: 100.
43. Love, W. D., and G. E. Burch. 1957. Differences in the rate of Rb^{86} uptake by several regions of the myocardium of control dogs and dogs receiving l-norepinephrine or pitressin. *J. Clin. Invest.* **36**: 479.
44. Sarnoff, S. J., E. Braunwald, G. H. Welch, Jr., R. B. Case, W. N. Stainsby, and R. Mancruz. 1958. Hemodynamic determinants of oxygen consumption of the heart with special reference to the tension-time index. *Amer. J. Physiol.* **192**: 148.
45. Haddy, F. J. 1969. Physiology and pharmacology of the coronary circulation and myocardium, particularly in relation to coronary artery disease. *Amer. J. Med.* **47**: 274.